NACA RM E9D12

RESEARCH MEMORANDUM

HEAT TRANSFER FROM HIGH-TEMPERATURE SURFACES TO FLUIDS III - CORRELATION OF HEAT-TRANSFER DATA FOR AIR FLOWING IN SILICON CARBIDE TUBE WITH ROUNDED ENTRANCE, INSIDE DIAMETER OF 3/4 INCH, AND EFFECTIVE LENGTH OF 12 INCHES

By Eldon W. Sams and Leland G. Desmon

Lewis Flight Propulsion Laboratory
Cleveland, Ohio

NATIONAL ADVISORY COMMITTEE FOR AERONAUTICS

WASHINGTON
June 23, 1949

NACA RM E9D12

NATIONAL ADVISORY COMMITTEE FOR AERONAUTICS

RESEARCH MEMORANDUM

HEAT TRANSFER FROM HIGH-TEMPERATURE SURFACES TO FLUIDS III - CORRELATION OF HEAT-TRANSFER DATA FOR AIR FLOWING IN SILICON CARBIDE TUBE WITH ROUNDED ENTRANCE, INSIDE DIAMETER OF 3/4 INCH, AND EFFECTIVE LENGTH OF 12 INCHES

By Eldon W. Sams and Leland G. Desmon

SUMMARY

A heat-transfer investigation was conducted with air flowing through an electrically heated silicon carbide tube with a rounded entrance, an inside diameter of 3/4 inch, and an effective heat-transfer length of 12 inches over a range of Reynolds numbers up to 300,000 and a range of average inside-tube-wall temperatures up to 2500° R. The highest corresponding local outside-tube-wall temperature was 3010° R.

Correlation of the heat-transfer data using the conventional Nusselt relation wherein physical properties of the fluid were evaluated at average bulk temperature resulted in a separation of data with tube-wall-temperature level. A satisfactory correlation of the heat-transfer data was obtained, however, by the use of modified correlation parameters wherein the mass velocity G (or product of average air density and velocity evaluated at bulk temperature $\rho_b V_b$) in the Reynolds number was replaced by the product of average air velocity evaluated at the bulk temperature and density evaluated at either the average inside-tube-wall temperature or the average film temperature; in addition, all the physical properties of air were correspondingly evaluated at either the average inside-tube-wall temperature or the average film temperature.

INTRODUCTION

A general program has been undertaken at the NACA Lewis laboratory to obtain surface-to-fluid forced-convection heat-transfer

data and associated information over a range of high surface temperatures and heat-flux densities.

As the first phase of the program, a heat-transfer investigation was conducted with air flowing through an electrically heated Inconel tube over a range of Reynolds numbers up to 250,000 and a range of average inside-tube-wall temperatures up to 1700° R, the results of which are reported in reference 1. Reference 2 enlarges upon the heat-transfer and associated data presented in reference 1 and extends the investigation to include ranges of Reynolds number up to 500,000 and average inside-tube-wall temperature up to 2050° R.

As a continuation of the general heat-transfer program, the investigation reported herein was conducted with air flowing through an electrically heated silicon carbide tube to obtain heat-transfer data over a greater range of surface temperature than was possible with the Inconel tube. Data were obtained over ranges of Reynolds number up to 300,000, average inside-tube-wall temperature up to 2500° R, heat-flux density up to 600,000 Btu per hour per square foot, and tube-exit Mach number up to 0.50. Average heat-transfer coefficients are correlated in accordance with the familiar Nusselt relation and with modifications thereto. Pressure-drop data are correlated with air flow and the ratio of tube-entrance- to tube-exit-air density.

APPARATUS

A schematic diagram of the heater tube and associated components of the air and electrical systems used in this investigation is shown in figure 1. A photograph of the heater-tube installation is shown in figure 2. The setup, in general, was similar to that of references 1 and 2.

Heater Tube

The heater tube, the details of which are shown in figure 3, consisted of a commercial silicon carbide tube having an inside diameter of 3/4 inch, a wall thickness of 3/16 inch, and a total length of 21 inches. The silicon carbide material used in the center 12-inch section of the heater tube had a higher resistivity than that used in the ends, thereby forming a continuous ceramic tube with a 12-inch hot section at the center (taken as the effective heat-transfer length) and a $4\frac{1}{2}$-inch cold section for terminal

connection at each end. Two braided-aluminum-wire terminal straps, clamped to the tube at each end, connected the heater tube to the electric power source.

An A.S.M.E. type long-radius low-ratio nozzle of the same throat diameter as the inside diameter of the tube was used to measure the air flow and also to provide a smooth air entrance into the heater tube. The heater tube was secured in position by two packing glands, one fastened to the nozzle plate at the tube entrance and the other to a plate at the tube exit.

The heater tube was thermally insulated by three concentric stainless-steel radiation shields with insulating cement filling the annular spaces between the shields. The total thickness of the insulation and shielding was $2\frac{1}{4}$ inches.

Outside-tube-wall temperatures were measured by 13 chromel-alumel thermocouples located at 1-inch intervals along the top of the 12-inch effective heat-transfer length and one additional thermocouple located 1/2 inch outside each end of the hot section. The thermocouples were cemented to the outside wall of the tube and wrapped a quarter turn around the tube to reduce conduction losses. Frequent inspection verified contact between the thermocouple junction and the tube wall. Temperatures were read by means of a manually operated potentiometer.

Air System

Air at a maximum pressure of about 50 pounds per square inch gage and a temperature of about 540° R was supplied through a pressure-regulating valve, air filter, air preheater, and a 0.620-inch A.S.M.E. type flat-plate orifice to a large surge tank, as indicated in figure 1. From the surge tank, the air passed through a calming tank, the tube-entrance flow nozzle, and the heater tube into the mixing tank where it was discharged to the atmosphere. The surge tank, calming tank, mixing tank, and entrance and exit piping adjoining the heater tube were thermally insulated.

The mixing tank contained three concentric tubes so arranged that the air leaving the heater tube made three axial passes through the mixing chamber before being discharged to the atmosphere. Two staggered baffles placed halfway through the innermost tube insured mixing of the heated air. The mixing tank was mounted on rollers to accomodate thermal expansion of the heater tube and was counterweighted to overcome rolling friction during thermal contraction of the tube.

The temperature of the air entering the heater tube was measured by two iron-constantan thermocouples located at the exit of the calming tank. The temperature of the air leaving the heater tube was measured by two chromel-alumel thermocouples located immediately downstream of the staggered baffles in the mixing chamber. Two static-pressure taps, one at the throat of the nozzle and the other in the tube-exit plate, were used to measure the pressure drop across the heater tube.

Electrical System

Power was supplied to the heater tube from a 208-volt 60-cycle alternating-current supply line stepped down to 120 volts through an autotransformer. A saturable reactor was connected in one of the power leads between the autotransformer and the heater tube. A rheostat, placed in the 125-volt direct-current supply line to the reactor, was used to control the degree of saturation of the reactor and corresponding power input to the heater tube. The capacity of the electric equipment was 15 kilovolt-amperes.

The power supplied to the heater tube was measured by a wattmeter. A voltmeter connected across the terminal straps and an ammeter connected in one of the copper power leads were used to measure voltage drop and current through the tube, respectively. The ammeter and current coil of the wattmeter were connected to the load through current transformers.

PRELIMINARY CALIBRATIONS AND EXPERIMENTAL PROCEDURE

Air-flow measurements. - Air-flow-calibration curves for the previously described long-radius low-ratio nozzle and the flat-plate orifice were calculated using established A.S.M.E. flow coefficients and equations available for these types of flow meter. The measured air flows, as indicated by the two individually calibrated meters, checked within 5 percent over the range investigated.

Tube-wall-temperature measurements. - In order to determine whether the outside-tube-wall temperatures (as indicated by the chromel-alumel thermocouples in contact with the wall) were affected by current flowing through the tube, power was supplied to the heater tube until a predetermined observed tube-wall temperature was reached and conditions were stabilized. The power was then shut off and the readings of several thermocouples were recorded at 5-second intervals. The temperature obtained by extrapolating the curve of the observed time-temperature readings to zero time for

each thermocouple was in agreement with the observed temperature reading just prior to the time of power shut off. The observed wall-temperature readings were therefore concluded to be insensitive to the 60-cycle current and to any stray fields that may have existed about the tube.

Leakage air-flow losses. - As a result of the process used in forming the silicon carbide tube, a certain amount of porosity existed in the heater-tube wall. A calibration of leakage air flow through the tube wall was therefore made over a range of average tube-wall temperatures and average static pressures in the tube. A predetermined pressure was established in the tube with the exit end closed (only leakage air flowing) and the air flow recorded for various values of average tube-wall temperature. The procedure was repeated for a range of average static pressures in the tube. The leakage air flow thus obtained for a given average tube-wall temperature and average static pressure in the tube was considered to be equivalent to that existing at the same temperature and pressure conditions during the heat-transfer runs.

The resulting calibration curve of the tube-wall leakage air flow is shown in figure 4 plotted against average outside-tube-wall temperature for a series of values of the ratio of average static pressure in the heater tube to atmospheric pressure p_t/p_a (where p_a is about 14.7 lb/sq in. absolute). For a constant value of p_t/p_a, the leakage air flow through the tube wall decreases with increasing tube-wall temperature. This trend may be accounted for by the fact that an increase in temperature causes both an increase in the viscosity of air and an increase in the grain size (with consequent reduction in porosity) of a ceramic.

External heat losses. - The external heat loss from the heater tube includes losses through radiation, conduction, and natural convection plus an additional heat loss effected by air leakage through the tube wall. An external-heat-loss calibration was made over a range of average tube-wall temperatures and a range of values of p_t/p_a in a manner similar to that used in determining leakage air flow. For a given tube-wall temperature and value of p_t/p_a (with only leakage air flowing), the power input to the tube was considered to be equivalent to the external heat loss existing at the same temperature and pressure conditions during the heat-transfer runs. The resulting calibration curve of the external heat loss plotted against average outside-tube-wall temperature is shown in figure 5 for a series of values of the ratio p_t/p_a.

Heat-transfer runs. - Surface-to-fluid heat-transfer coefficients and associated data were obtained over ranges of Reynolds number up to 300,000, average inside-tube-wall temperature up to 2500° R (local outside-tube-wall temperature reaching 3010° R), heat-flux density up to 600,000 Btu per hour per square foot, and exit Mach number up to 0.50.

The first silicon carbide heater tube used in this investigation failed after heat-transfer data were obtained up to an average inside-tube-wall temperature of 1675° R. A second tube, having the same composition and physical dimensions as the first, was instrumented and installed in the setup. Data on the second tube were obtained at average inside-tube-wall temperatures of 785°, 1161°, 1722°, 2125°, and 2502° R.

In establishing a test condition, the tube-entrance air pressure was set at the minimum value that could be obtained with the pressure-regulating valve; power was then supplied to the heater tube until the desired average inside-tube-wall temperature was obtained and stabilized. All temperature, pressure, and power-input readings were then recorded. The procedure was repeated for successive air flows throughout the desired range of Reynolds number for the same average tube-wall temperature.

SYMBOLS

The following symbols are used in the calculations:

A	cross-sectional area of fluid stream, 0.00307 (sq ft)
c_p	specific heat of air at constant pressure, (Btu/(lb)(°F))
D	inside diameter of heater tube, (ft)
G	mass velocity, W_{corr}/A, (lb/(hr)(sq ft))
H_l	external heat loss, (Btu/hr)
h	average heat-transfer coefficient, (Btu/(hr)(sq ft)(°F))
k	thermal conductivity of air, (Btu/(hr)(sq ft)(°F/ft))
k_t	thermal conductivity of tube material (silicon carbide), (Btu/(hr)(sq ft)(°F/ft))
L	effective heat-transfer length of heater tube, (ft)

Δp	static-pressure drop through heater tube, (lb/sq ft)
p_t/p_a	ratio of average static pressure in heater tube to atmospheric pressure
Q	rate of heat transfer to air, (Btu/hr)
r_i	inner radius of heater tube, (ft)
r_o	outer radius of heater tube, (ft)
S	effective heat-transfer area of heater tube, 0.1965 (sq ft)
T_b	air bulk temperature (average total air temperature), $1/2\ (T_1 + T_2)$, ($^\circ$R)
T_f	average film temperature, $1/2\ (T_b + T_s)$, ($^\circ$R)
T_o	average outside-tube-wall temperature, ($^\circ$R)
T_s	average inside-tube-wall temperature (surface temperature), ($^\circ$R)
T_1	total air temperature at heater-tube entrance, ($^\circ$R)
T_2	total air temperature at heater-tube exit, ($^\circ$R)
V	velocity of air, (ft/hr)
W_{corr}	corrected air flow, $W_t - \frac{1}{2}W_l$, (lb/hr)
W_l	tube-wall leakage air flow, (lb/hr)
W_t	total air flow at tube entrance, (lb/hr)
μ	absolute viscosity of air, (lb/(hr)(ft))
ρ	density of air, (lb/cu ft)
ρ_1/ρ_2	ratio of air densities at entrance and exit of heater tube
σ_1	ratio of air density at tube entrance to standard sea-level air density, $\rho_1/0.0765$
$\frac{hD}{k}$	Nusselt number

$\frac{c_p\mu}{k}$ Prandtl number

$\frac{DG}{\mu}$ Reynolds number, $\frac{\rho_b V_b D}{\mu_b}$

$\frac{\rho_f V_b D}{\mu_f}$ modified film Reynolds number

$\frac{\rho_s V_b D}{\mu_s}$ modified surface Reynolds number

Subscripts:

b physical properties of air evaluated at air bulk temperature T_b

f physical properties of air evaluated at average film temperature T_f

s physical properties of air evaluated at average inside-tube-wall temperature T_s

METHODS OF CALCULATION

Temperatures. - The average outside-tube-wall temperature T_o was obtained by measuring the area under a curve of the temperature distribution along the effective heat-transfer length (as obtained from thermocouple readings) and dividing the area by the effective heat-transfer length.

The average inside-tube-wall temperature T_s was then calculated from the average outside-tube-wall temperature, the rate of heat transfer to air, and the thermal conductivity and physical dimensions of the heater tube by the following equation (derived in reference 3):

$$T_s = T_o - \frac{Q}{2\pi L\, k_t\, (r_o^2 - r_i^2)} \left(r_o^2 \log_e \frac{r_o}{r_i} - \frac{r_o^2 - r_i^2}{2} \right)$$

In the foregoing equation, the assumption is made that heat is generated uniformly across the tube-wall thickness and the heat flow from every point in the tube wall is radially inward. Substituting the values for thermal conductivity of silicon carbide (assumed constant) and physical dimensions of the heater tube reduces the equation to

$$T_s = T_o - 0.00368\ Q$$

A value of 10.0 was used for the thermal conductivity of silicon carbide because of the lack of data on its variation with temperature. The possible error introduced is negligible inasmuch as the calculated temperature drop across the tube-wall thickness is small compared with the difference between the average inside-tube-wall and the air bulk temperatures.

The air bulk temperature was taken as the average of the heater-tube entrance and exit total-air temperatures T_1 and T_2, respectively. The average film temperature T_f was taken as the average of the air bulk temperature and the average inside-tube-wall temperature.

Heat-transfer coefficient. - The average heat-transfer coefficient h was calculated by the following equation:

$$h = \frac{W_{corr}\, c_{p,b}\, (T_2 - T_1)}{S\, (T_s - T_b)}$$

The air-flow term W_{corr} used in this equation included a correction for the air leakage through the heater-tube wall. For a given condition, only one-half of the leakage air entering the tube was assumed to be effectively heated to the exit total-air temperature T_2; the corrected air flow W_{corr} was therefore taken as the total flow entering the tube W_t less one-half the corresponding tube-wall leakage flow W_l as determined from figure 4. The maximum value of tube-wall leakage flow encountered during the heat-transfer runs was less than 10 percent of the total flow entering the tube.

Physical properties of air. - The values used herein of specific heat at constant pressure c_p, thermal conductivity k, absolute viscosity μ, and corresponding values of Prandtl

number $c_p\mu/k$ for air were obtained from references 4 and 5 and are plotted in figure 6 as a function of temperature. The data of reference 4 covered a temperature range from 351° to 2060° R and were the same as the data used in the investigations of references 1 and 2. The data corresponding to temperatures from 2060° to 2600° R were obtained from reference 5 and were slightly adjusted at the low-temperature end to provide continuity with the data of reference 4.

RESULTS AND DISCUSSION

Tube-Wall-Temperature Distribution

Axial-temperature-distribution curves showing the outside-tube-wall temperature along the effective heat-transfer length of the heater tube for the condition of no air flow are presented in figure 7 for various values of electric heat input and corresponding average outside-tube-wall temperature. The steep temperature gradients at the entrance and exit of the hot section are a result of the heat-conduction losses through the terminal straps and tube-end supporting plates. The curves are approximately symmetrical about the center of the hot section.

Representative outside-tube-wall-temperature-distribution curves for the condition of air flowing through the tube are shown in figure 8 for five values of electric heat input and resulting average outside-tube-wall temperature. Figures 8(a) and 8(b) are for nominal Reynolds numbers of 47,500 and 157,000, respectively, based on the air bulk temperature. The curves indicate a shift of the peak temperature toward the tube exit with an increase in Reynolds number. A steep temperature gradient, similar to that for the no-flow condition (fig. 7), exists at each end of the hot section.

Heat Balance

A heat balance for the heat-transfer runs conducted on both the first and second silicon carbide tubes is shown in figure 9 wherein the value for rate of heat transfer to air plus the external heat loss (obtained from fig. 5), $(W_t - W_l)c_{p,b}(T_2 - T_1) + H_l$ is plotted against the corresponding value of electric heat input. Inasmuch as the value of external heat loss, as obtained from figure 5, includes the heat lost to the leakage air, the total air

flow W_t less the leakage flow W_l was used to evaluate the corresponding rate of heat transferred to air for use in the heat balance. The heat-balance data have a maximum deviation of about 5 percent from the match line.

Correlation of Heat-Transfer Coefficients

Inasmuch as the data obtained with the first tube were incomplete (because of tube failure), only the data obtained with the second heater tube are presented in the development of a satisfactory heat-transfer correlation. The data for the first tube, however, are included for comparison in the final correlation method.

Correlation based on air bulk temperature. - The data of this investigation are presented in figure 10 in accordance with the conventional correlation method wherein Nusselt number divided by Prandtl number raised to the 0.4 power $\left(hD/k_b\right)\Big/\left(\frac{c_{p,b}\,\mu_b}{k_b}\right)^{0.4}$ is plotted against Reynolds number DG/μ_b with the physical properties of air evaluated at the air bulk temperature.

A family of parallel lines representing the five average inside-tube-wall-temperature levels investigated and having slopes of about 0.82 at Reynolds numbers above approximately 40,000 were obtained. At lower Reynolds numbers, the data fall off indicating the presence of transition flow. The values of the heat-transfer parameter $\left(hD/k_b\right)\Big/\left(\frac{c_{p,b}\,\mu_b}{k_b}\right)^{0.4}$ decrease progressively with an increase in tube-wall temperature; the value at 2502° R is about 35 percent lower than that obtained at 785° R at a Reynolds number of 70,000. A decrease in the value of the heat-transfer parameter with an increase in tube-wall temperature was also observed in the data of references 1 and 2. Included for comparison is the line (dashed) obtained from reference 6, wherein the results of various investigators were correlated using the same values of physical properties of air as were used herein (fig. 6). The reference line was obtained by transposing data from a Stanton number plot in reference 6 to the coordinates of figure 10 with the Prandtl number assigned a value of 0.70, which corresponds to the physical properties of air at 580° R (fig. 6). The low-temperature data of references 1 and 2 (not shown) were in agreement with the line of

reference 6, whereas the low-temperature data of this investigation fall above the line of reference 6.

This discrepancy may be due to one or more of the following factors that must be taken into consideration in evaluating the present data:

1. As previously mentioned, the surface area S used in calculating the average heat-transfer coefficient h included only the area of the high-resistance section of the tube. Inasmuch as the end sections contributed an indeterminable amount to the total heat transferred, the calculated values of the heat-transfer coefficients may be different from the actual values.

2. In view of the large difference between the tube-wall and air-temperature distributions along the tube length, the average heat-transfer coefficient h calculated from the difference between the average wall and average air temperatures may not be a true average of the local heat-transfer coefficients.

3. Increased turbulence resulting from a high degree of roughness of the tube wall may result in higher than normal heat-transfer coefficients.

4. Bleeding off of the boundary layer as a result of air leakage through the tube wall may result in higher than normal heat-transfer coefficients.

Correlation based on surface temperature. - The data are replotted in figure 11 with the physical properties of air evaluated at the average inside-tube-wall temperature (surface temperature). The lines through the data representing the five wall-temperature levels show the same general characteristics as pointed out in figure 10; in this case, however, the separation of data for the same range of wall temperatures is greater, the value of

$$\left(hD/k_s\right)\Big/\left(\frac{c_{p,s}\,\mu_s}{k_s}\right)^{0.4}$$

at 2502° R being about 50 percent lower than that obtained at 785° R at a Reynolds number of 70,000. If the physical properties of air were evaluated at the average film temperature, the separation of data for the same increase in wall temperatures would be between the 35-percent and 50-percent decrease in values indicated in figures 10 and 11.

Correlation based on modified surface Reynolds number. - The heat-transfer data are replotted in figure 12 wherein the mass

velocity G (or $\rho_b V_b$) in the conventional (or bulk) Reynolds number is replaced by the product of air density evaluated at the average inside-tube-wall temperature ρ_s and average velocity evaluated at the bulk temperature V_b; in addition, all the physical properties of air are evaluated at the average inside-tube-wall temperature. This modified surface Reynolds number is related to the conventional Reynolds number by the following equation:

$$\frac{\rho_s V_b D}{\mu_s} = \left(\frac{DG}{\mu_s}\right)\left(\frac{\rho_s}{\rho_b}\right) = \left(\frac{DG}{\mu_b}\right)\left(\frac{\mu_b}{\mu_s}\right)\left(\frac{T_b}{T_s}\right)$$

This method of plotting (fig. 12) results in a satisfactory correlation of the data for the five tube-wall-temperature levels investigated although a slight temperature effect still exists. The slope of the line drawn through the data above a Reynolds number of approximately 10,000 is 0.83.

Included for comparison is the line (dashed) from reference 1 that was obtained by the same method and correlates heat-transfer data from a similar setup (using an Inconel tube) for ranges of inside-tube-wall temperature up to 1700° R and Reynolds number above 10,000. The slope of the reference line is 0.80. The higher heat-transfer coefficients obtained in this investigation as compared with those shown by the reference correlation line may again be accounted for by one or more of the factors mentioned in the discussion of figure 10. For these reasons, it is believed that the results of reference 1 are more accurate than the results presented herein. The results of this investigation are of interest, however, in that they indicate that the method of correlation based on the average inside-tube-wall temperature still applies up to tube-wall temperatures of 2500° R, the limit of this investigation.

Correlation based on modified film Reynolds number. - The data are replotted in figure 13 wherein the mass velocity G (or $\rho_b V_b$) in the Reynolds number is replaced by the product of air density evaluated at the average film temperature ρ_f and average velocity evaluated at the bulk temperature V_b; in addition, all the physical properties of air are evaluated at the average film temperature. The relation between the modified film Reynolds number and the conventional Reynolds number is given by the following equation:

$$\frac{\rho_f V_b D}{\mu_f} = \left(\frac{DG}{\mu_f}\right)\left(\frac{\rho_f}{\rho_b}\right) = \left(\frac{DG}{\mu_b}\right)\left(\frac{\mu_b}{\mu_f}\right)\left(\frac{T_b}{T_f}\right)$$

This method of plotting (fig. 13) results in a good correlation of the data over the ranges of average inside-tube-wall temperature and Reynolds number investigated. This correlation is better than that obtained using the modified surface Reynolds number (fig. 12) for the present data. For the data of reference 1, however, the modified surface correlation proved slightly better than the modified film correlation. The results of the investigation reported herein are not considered sufficiently accurate to serve as a basis in choosing between the average film temperature and the average inside-tube-wall temperature for evaluation of the physical properties of air in the correlation equation.

For purposes of comparison, the data of figure 13 are replotted in figure 14 with additional heat-transfer data obtained on the first heater tube. This method of plotting (modified film Reynolds number) also correlates the data for the first tube throughout the range of tube-wall temperatures investigated, the slope of the correlation line (dashed) being 0.75. The difference in slope between the two correlation lines, which becomes apparent at Reynolds numbers above 20,000, is not clearly understood, but may be partly due to inherent differences in tube-wall roughness.

Pressure-Drop Correlation

Measured values of static-pressure drop through the second heater tube are correlated in figure 15 where the product of the ratio of air density at tube entrance to standard sea-level density σ_1 and the pressure drop through the tube Δp divided by corrected air flow to the 1.86 power $W_{corr}{}^{1.86}$ is plotted against the ratio of air densities at the entrance and exit of the heater tube ρ_1/ρ_2. The exponent 1.86 on corrected air flow was obtained from logarithmic plots of $\sigma_1 \Delta p$ against W_{corr} for constant values of ρ_1/ρ_2. The densities ρ_1/ρ_2 were evaluated at the static pressure and total temperature at the entrance and exit of the tube, respectively. The pressure-drop data correlate within a maximum deviation of ± 10 percent.

SUMMARY OF RESULTS

The results of the heat-transfer investigation with air flowing through an electrically heated silicon carbide tube with a rounded entrance, an inside diameter of 3/4 inch, and an effective heat-transfer length of 12 inches for ranges of Reynolds number up to 300,000 and average inside-tube-wall temperature up to 2500° R (corresponding local outside-tube-wall temperature reaching 3010° R) showed that:

1. Correlation of average heat-transfer coefficients using the conventional Nusselt relation, wherein physical properties of the fluid are evaluated at the air bulk temperature, resulted in a separation of data with tube-wall-temperature level; at a Reynolds number of 70,000, the Nusselt number decreased about 35 percent with an increase in average inside-tube-wall temperature from 785° to 2502° R. A similar effect resulted when the physical properties of air were evaluated at the average inside-tube-wall temperature, although in this case the Nusselt number decreased about 50 percent for the same increase in average tube-wall temperature.

2. A satisfactory correlation of the heat-transfer data over the ranges of inside-tube-wall temperature and Reynolds number investigated was obtained by the use of modified correlation methods wherein the mass velocity G (or product of average air density and velocity evaluated at bulk temperature $\rho_b V_b$) in the Reynolds number was replaced by the product of average velocity evaluated at the bulk temperature and density evaluated at either the average inside-tube-wall temperature or the average film temperature; in addition, all the physical properties of air were correspondingly evaluated at either the average inside-tube-wall temperature or the average film temperature. The correlation based on the average film temperature was somewhat better than that based on the average inside-tube-wall temperature. Because of uncertainties in evaluation of the heat-transfer coefficients, such as the bleeding off of the boundary layer, the results of this investigation are not considered sufficiently accurate to serve as a basis in choosing between the average film temperature and the average inside-tube-wall temperature for evaluation of the physical properties of air in the correlation equation.

Lewis Flight Propulsion Laboratory,
National Advisory Committee for Aeronautics,
Cleveland, Ohio.

REFERENCES

1. Humble, Leroy V., Lowdermilk, Warren H., and Grele, Milton: Heat Transfer from High-Temperature Surfaces to Fluids. I - Preliminary Investigation with Air in Inconel Tube with Rounded Entrance, Inside Diameter of 0.4 Inch, and Length of 24 Inches. NACA RM E7L31, 1948.

2. Lowdermilk, Warren H., and Grele, Milton D.: Heat Transfer from High-Temperature Surfaces to Fluids. II - Correlation of Heat-Transfer and Friction Data for Air Flowing in Inconel Tube with Rounded Entrance. NACA RM E8L03, 1949.

3. Bernardo, Everett, and Eian, Carroll S.: Heat-Transfer Tests of Acqueous Ethylene Glycol Solutions in an Electrically Heated Tube. NACA ARR E5F07, 1945.

4. Tribus, Myron, and Boelter, L. M. K.: An Investigation of Aircraft Heaters. II - Properties of Gases. NACA ARR, Oct. 1942.

5. Keenan, Joseph H., and Kaye, Joseph: Thermodynamic Properties of Air. John Wiley & Sons, Inc., 1945.

6. Drexel, Roger E., and McAdams, William H.: Heat-Transfer Coefficients for Air Flowing in Round Tubes, in Rectangular Ducts, and around Finned Cylinders. NACA ARR 4F28, 1945.

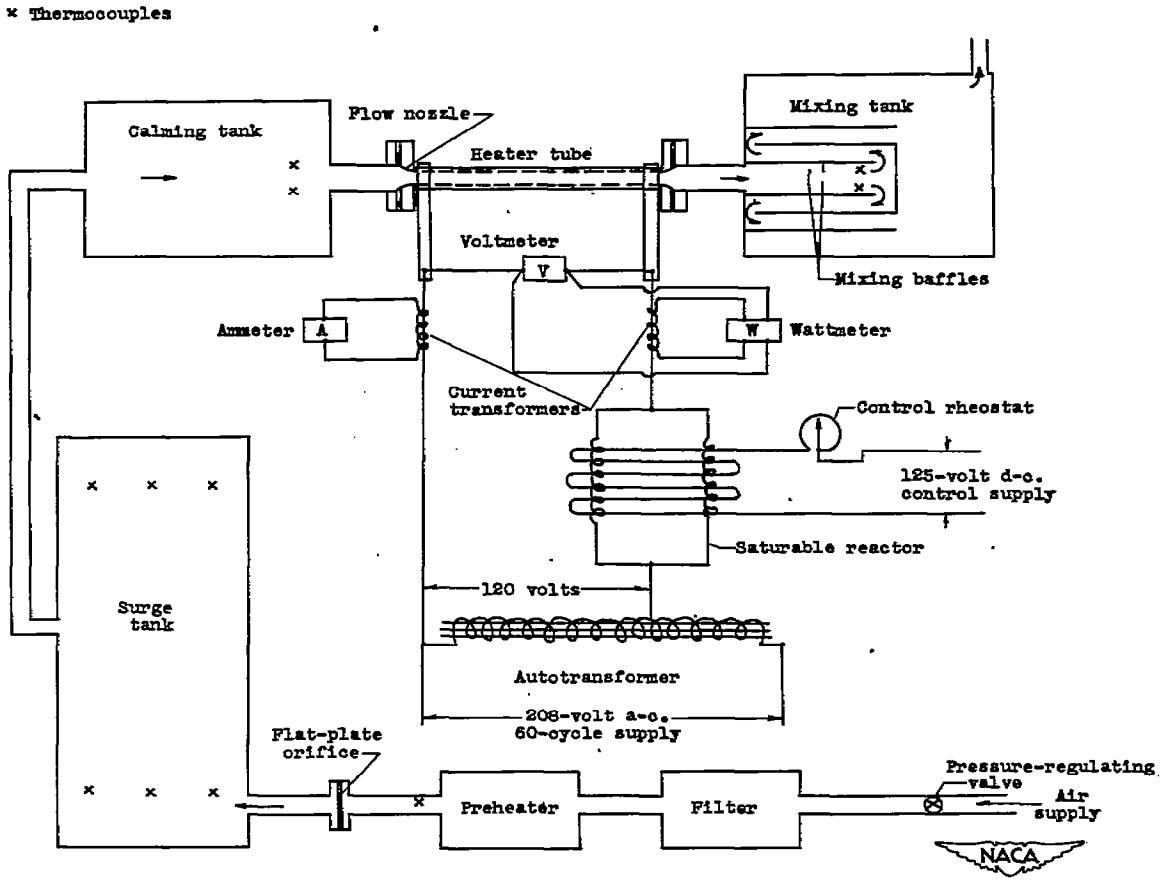

Figure 1. - Schematic diagram showing arrangement of experimental equipment.

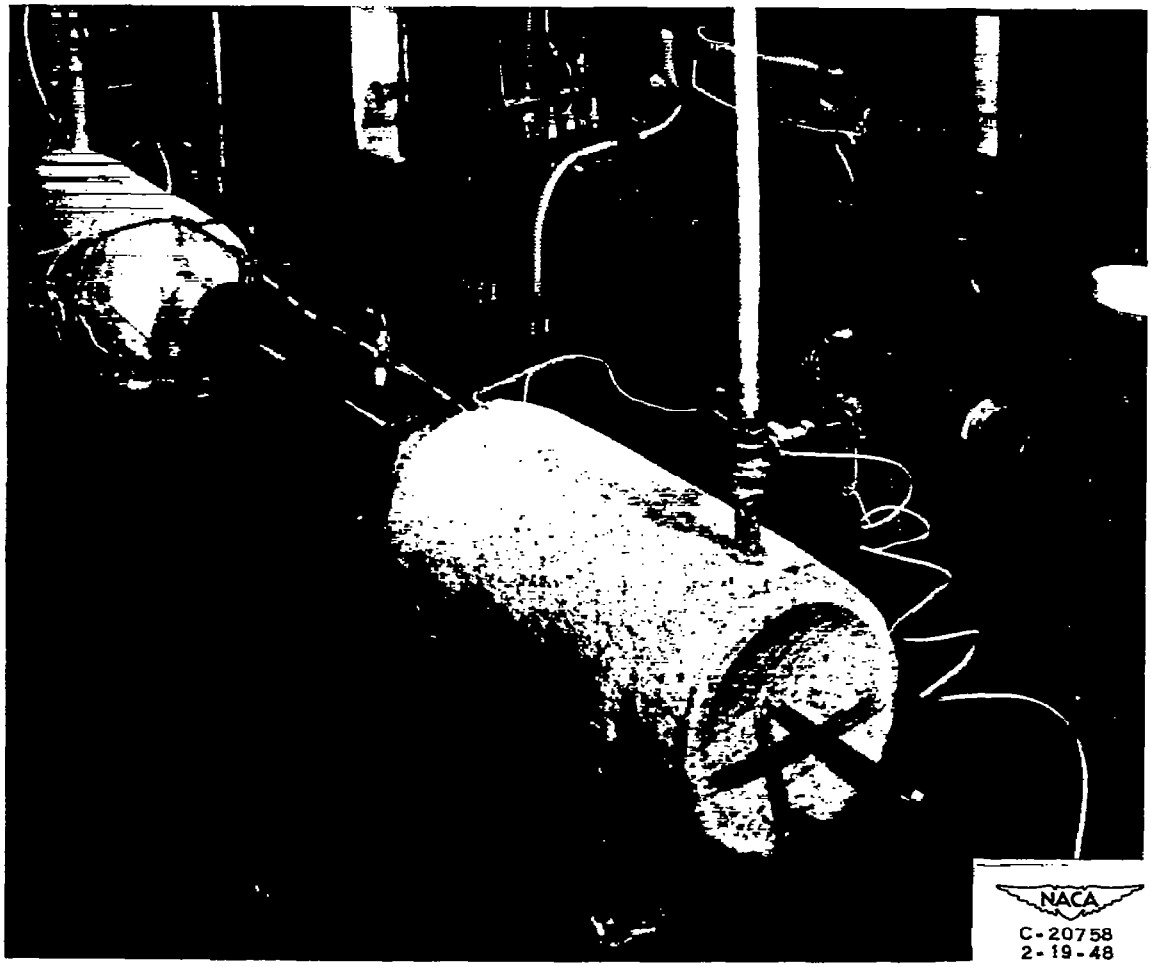

Figure 2. - General view of heater-tube installation.

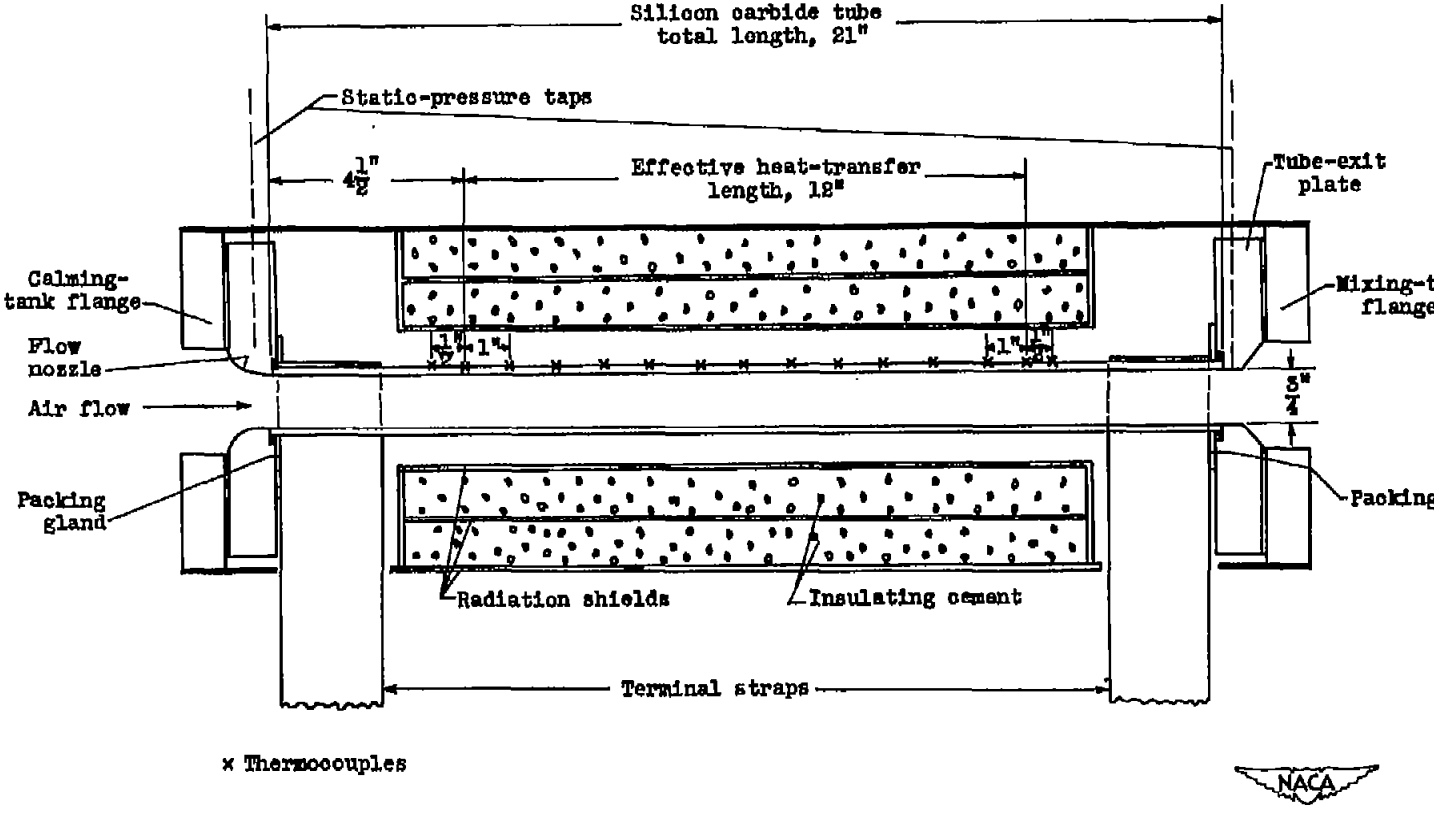

Figure 3. - Schematic diagram of heater tube showing thermocouple and pressure-tap locations.

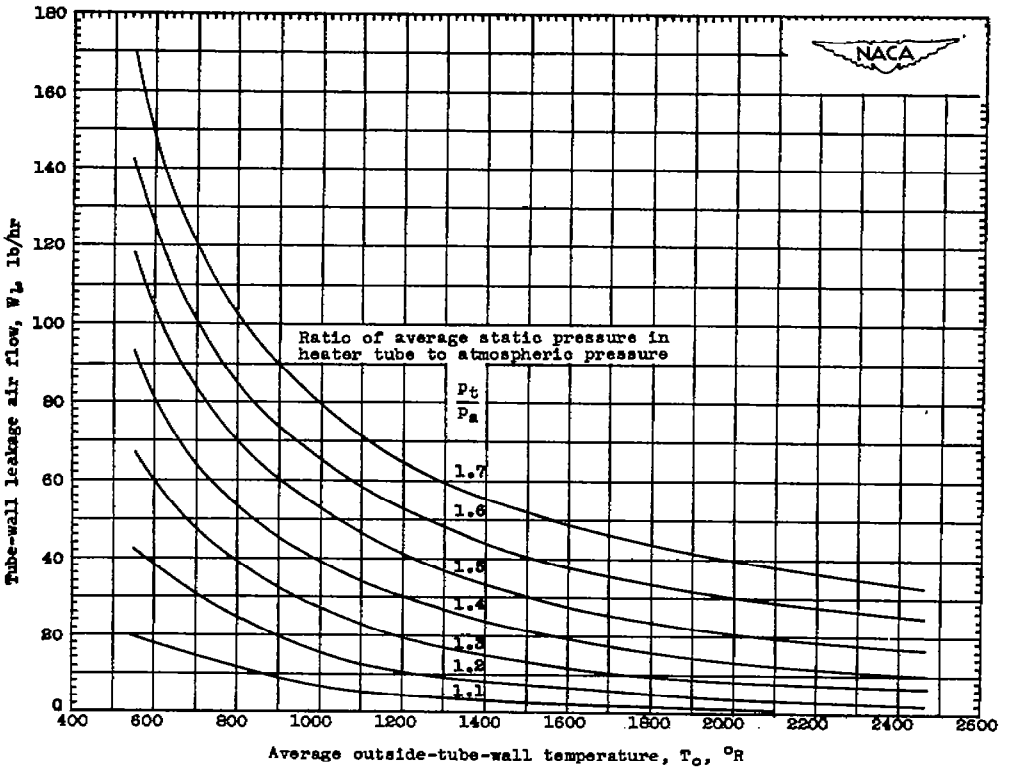

Figure 4. - Variation of tube-wall leakage air flow with average outside-tube-wall temperature for various values of ratio of average static pressure in heater tube to atmospheric pressure. Atmospheric pressure, 14.7 pounds per square inch absolute.

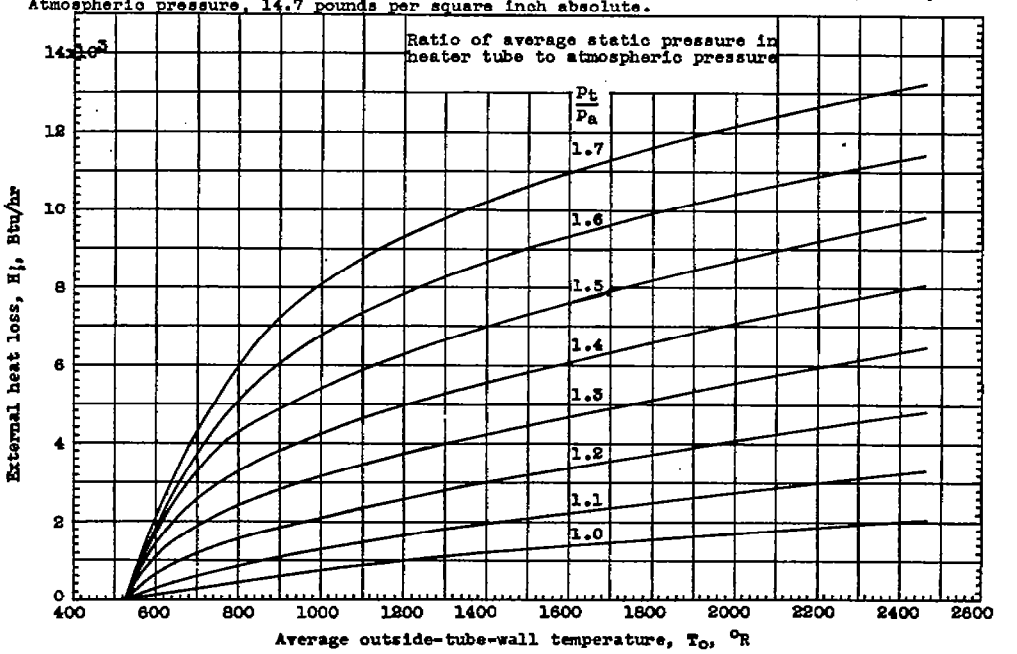

Figure 5. - Variation of external heat loss with average outside-tube-wall temperature for various values of ratio of average static pressure in heater tube to atmospheric pressure. Atmospheric pressure, 14.7 pounds per square inch absolute.

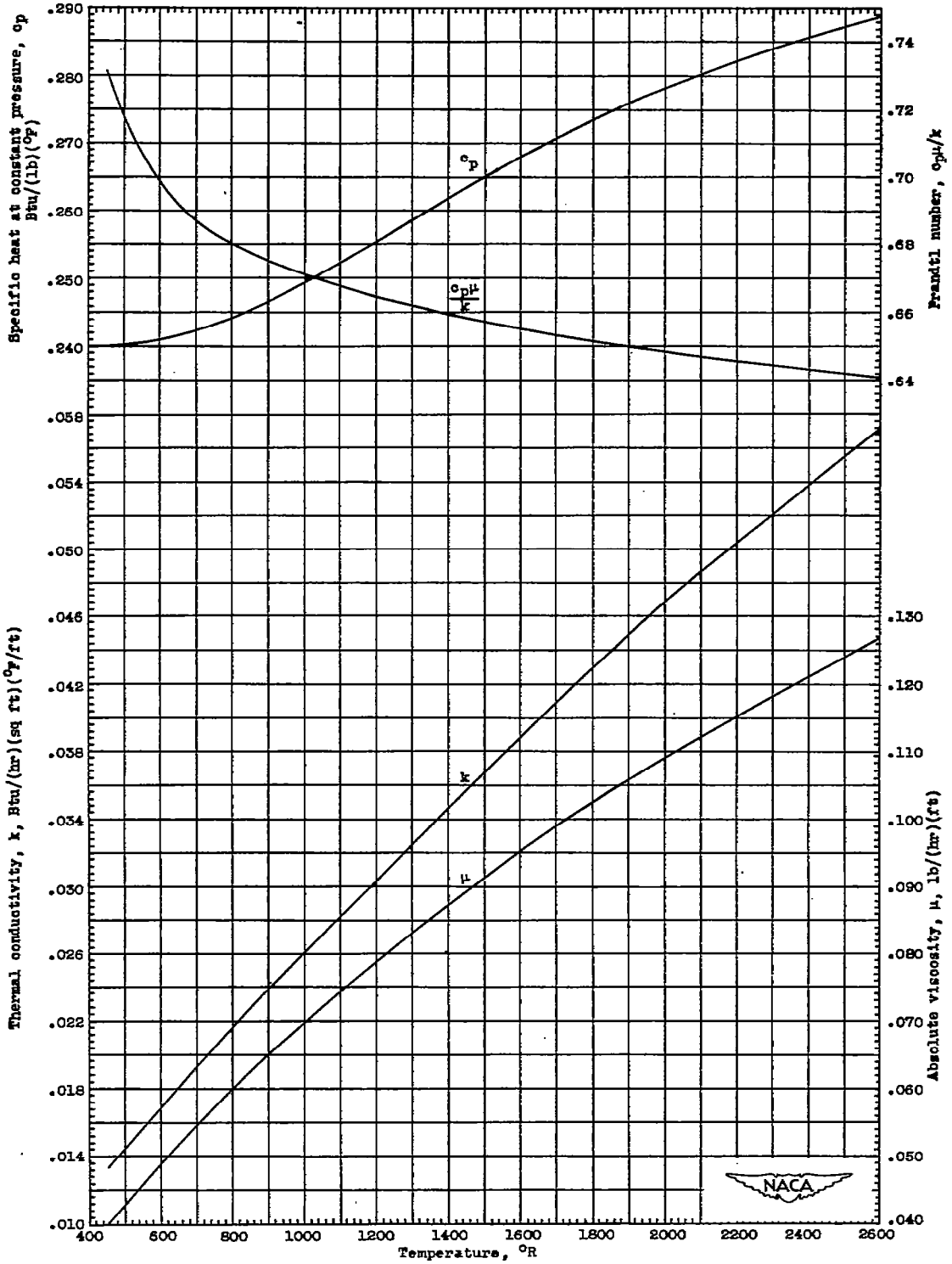

Figure 6. - Variation of specific heat at constant pressure, thermal conductivity, absolute viscosity, and Prandtl number of air with temperature. (Data from references 4 and 5.)

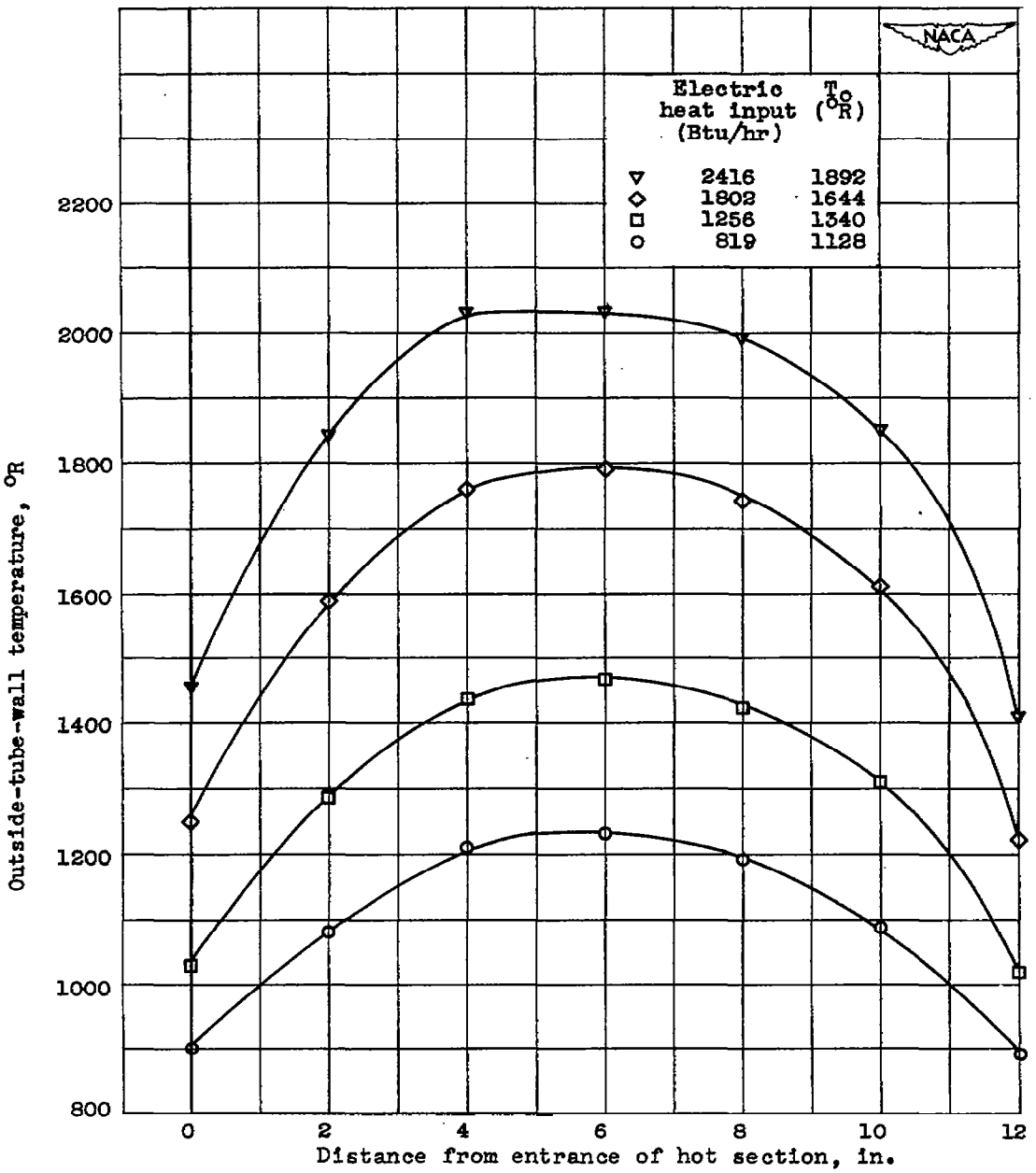

Figure 7. - Outside-tube-wall-temperature distribution along effective heat-transfer length for various amounts of electric heat input with no air flow.

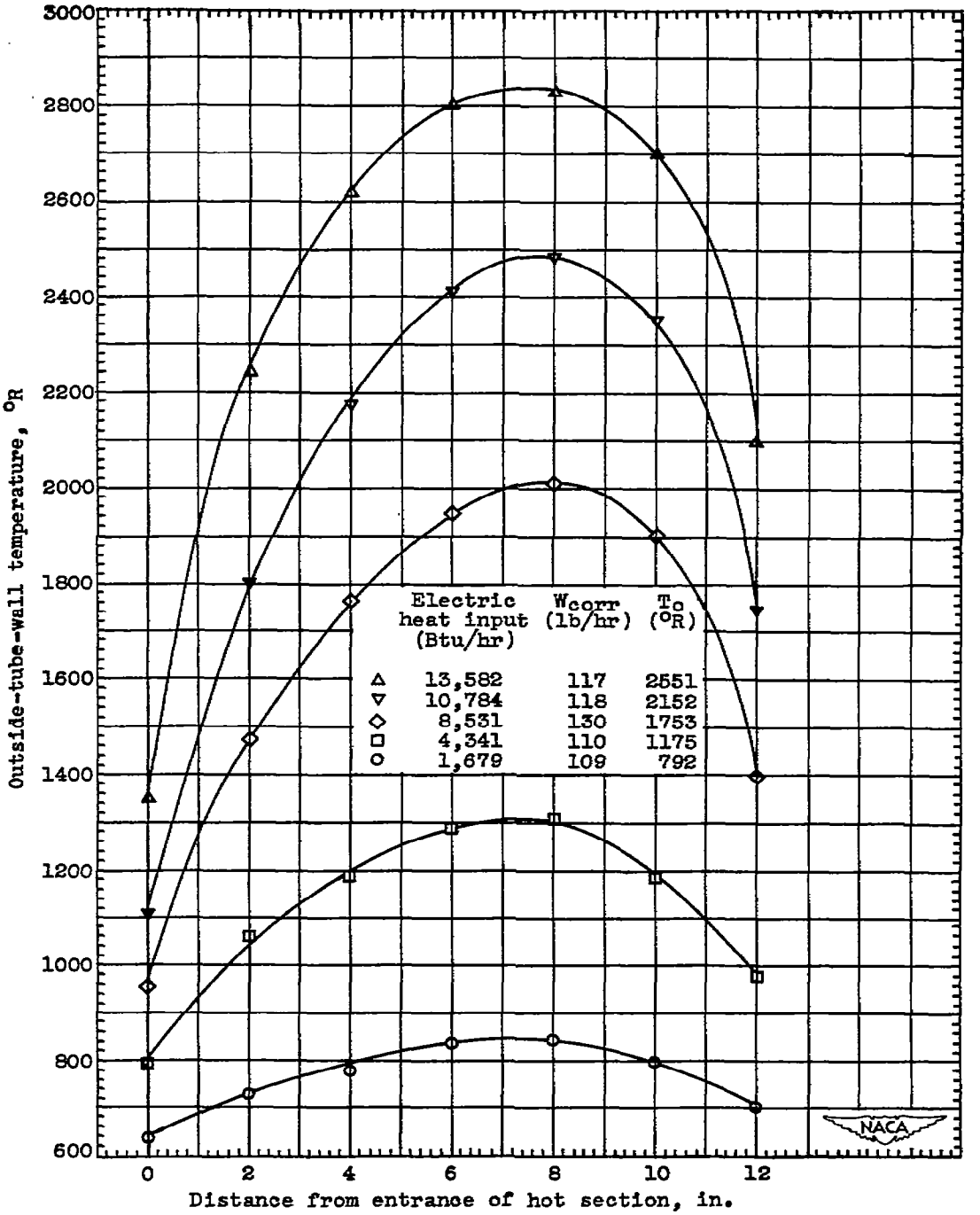

(a) Nominal Reynolds number, 47,500.

Figure 8. - Outside-tube-wall-temperature distribution along effective heat-transfer length for various amounts of electric heat input and constant values of Reynolds number.

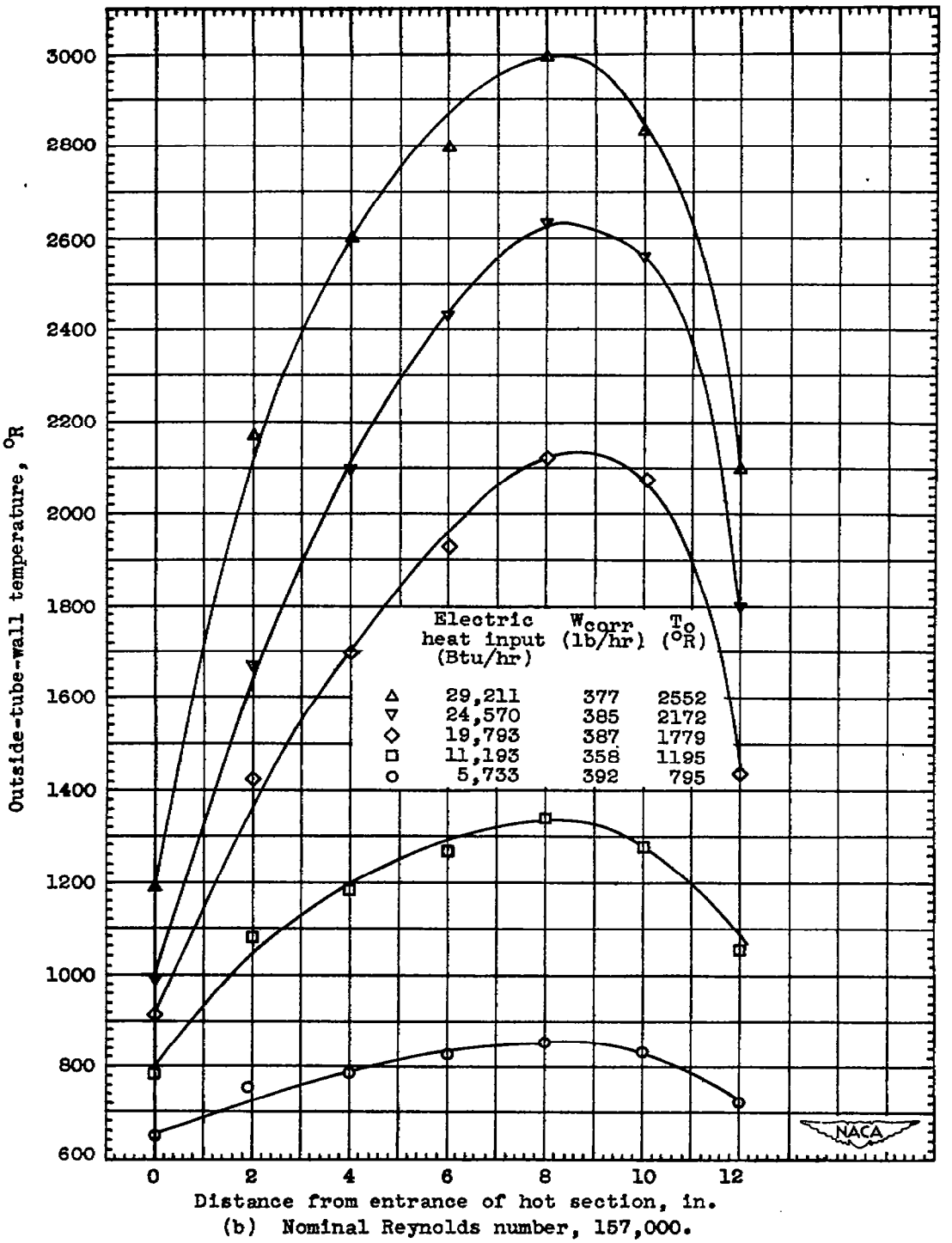

(b) Nominal Reynolds number, 157,000.

Figure 8. - Concluded. Outside-tube-wall-temperature distribution along effective heat-transfer length for various amounts of electric heat input and constant values of Reynolds number.

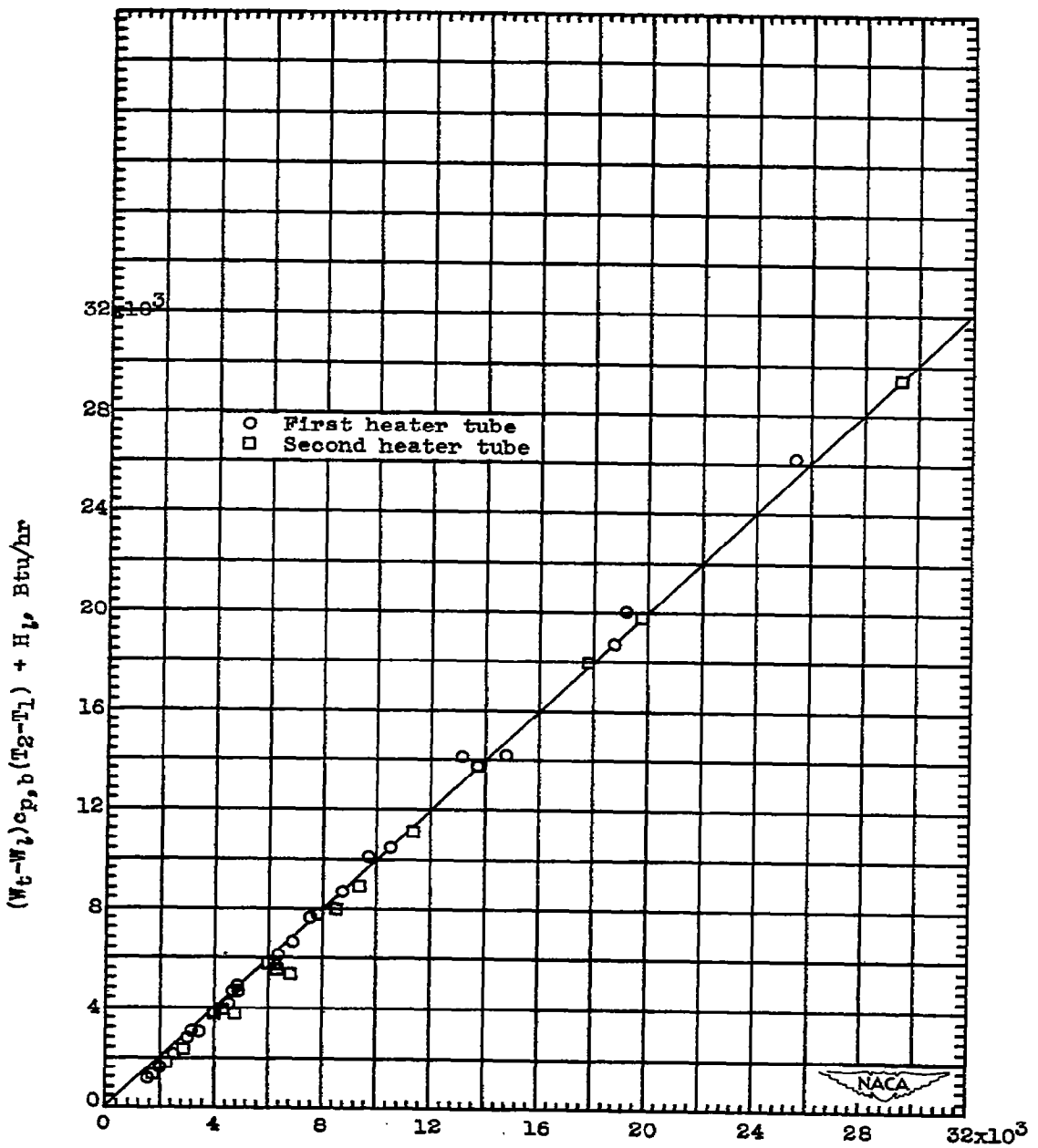

Figure 9. - Heat balance.

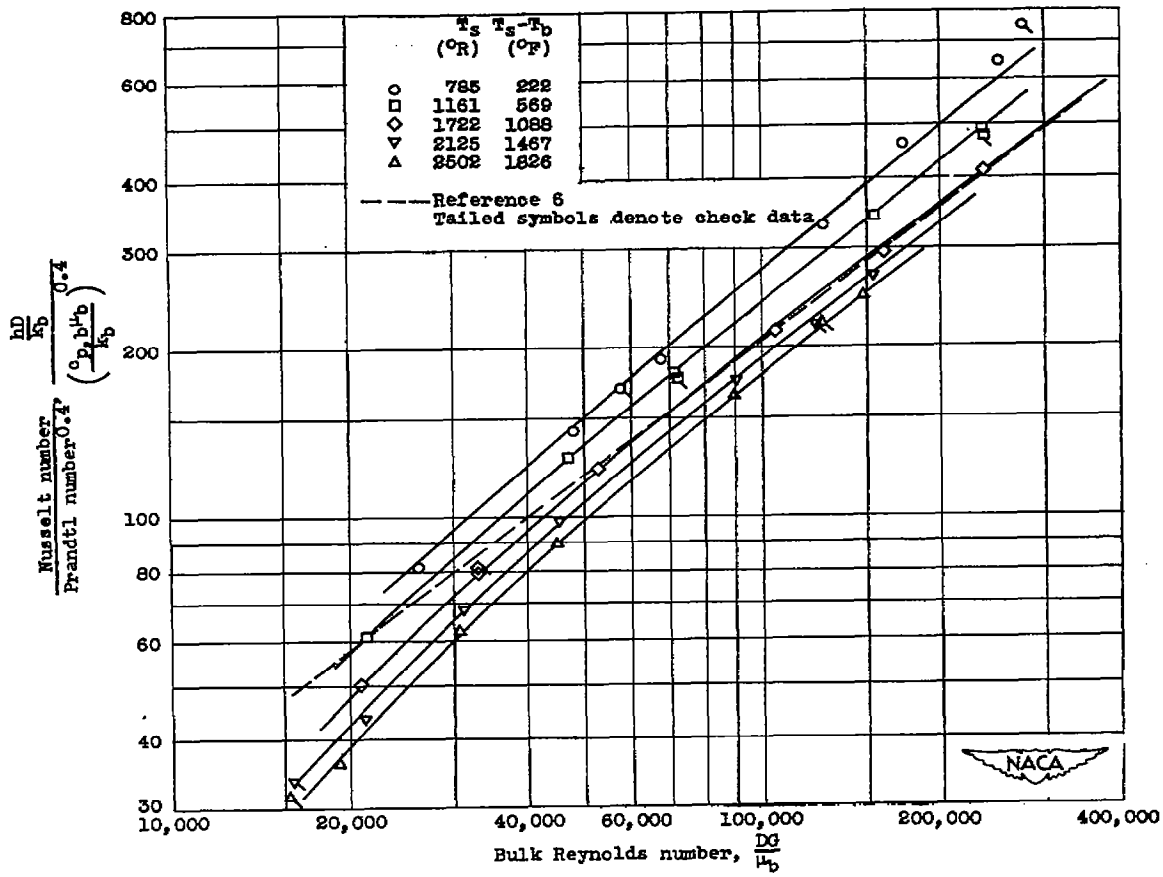

Figure 10. - Correlation of heat-transfer data. Physical properties of air evaluated at air bulk temperature T_b.

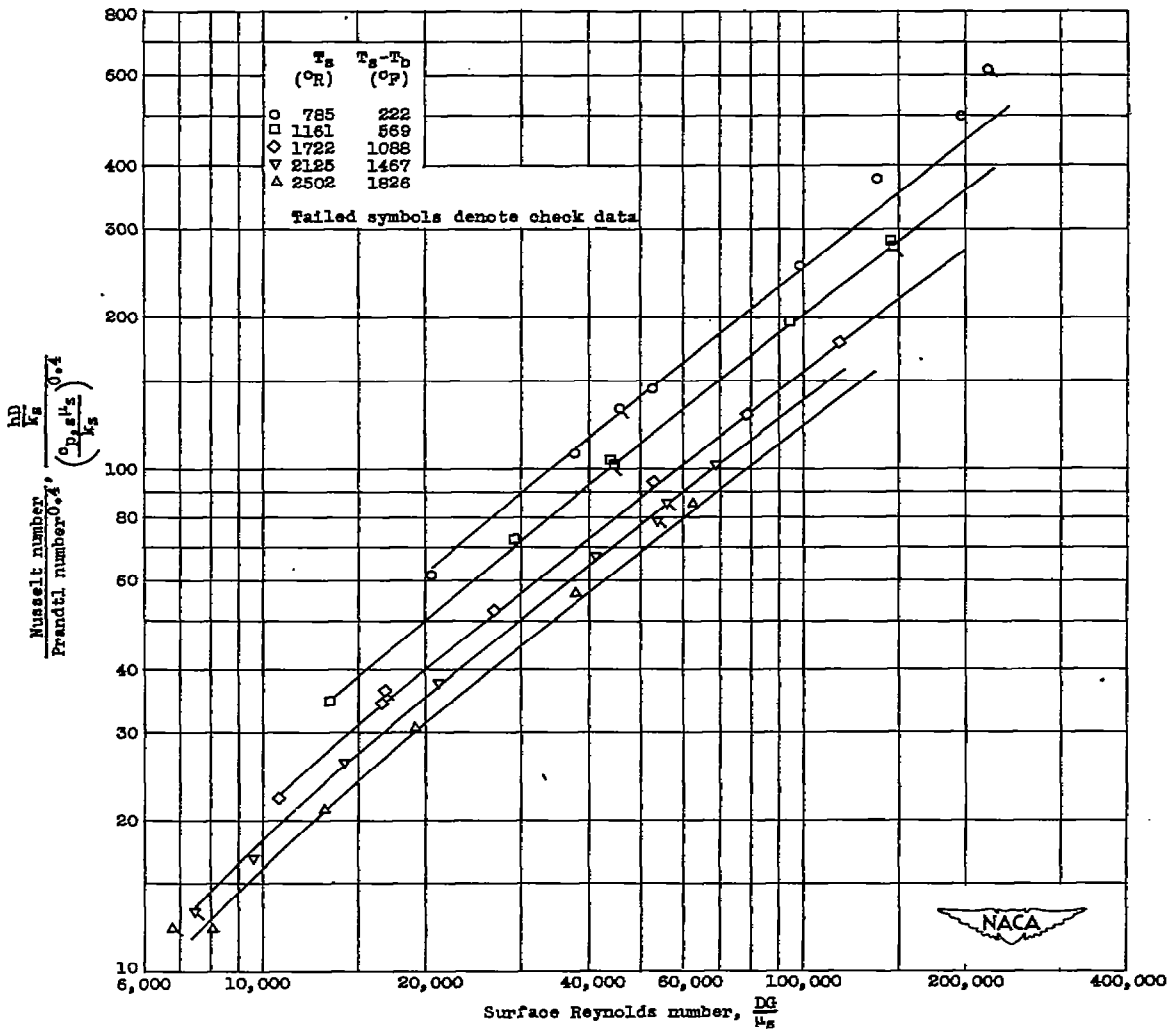

Figure 11. - Correlation of heat-transfer data. Physical properties of air evaluated at average surface temperature T_s.

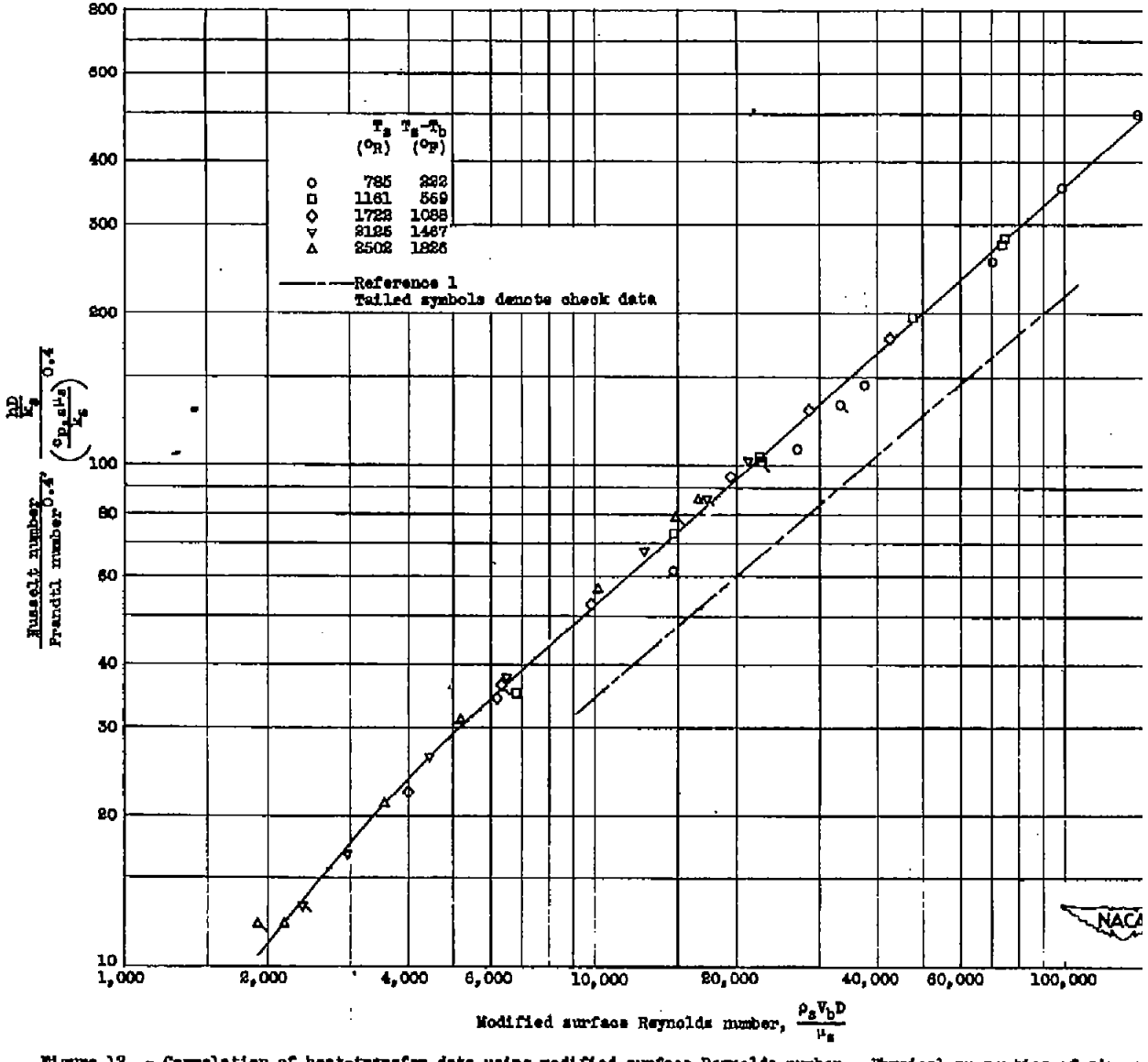

Figure 13. - Correlation of heat-transfer data using modified surface Reynolds number. Physical properties of air ev at average surface temperature T_s.

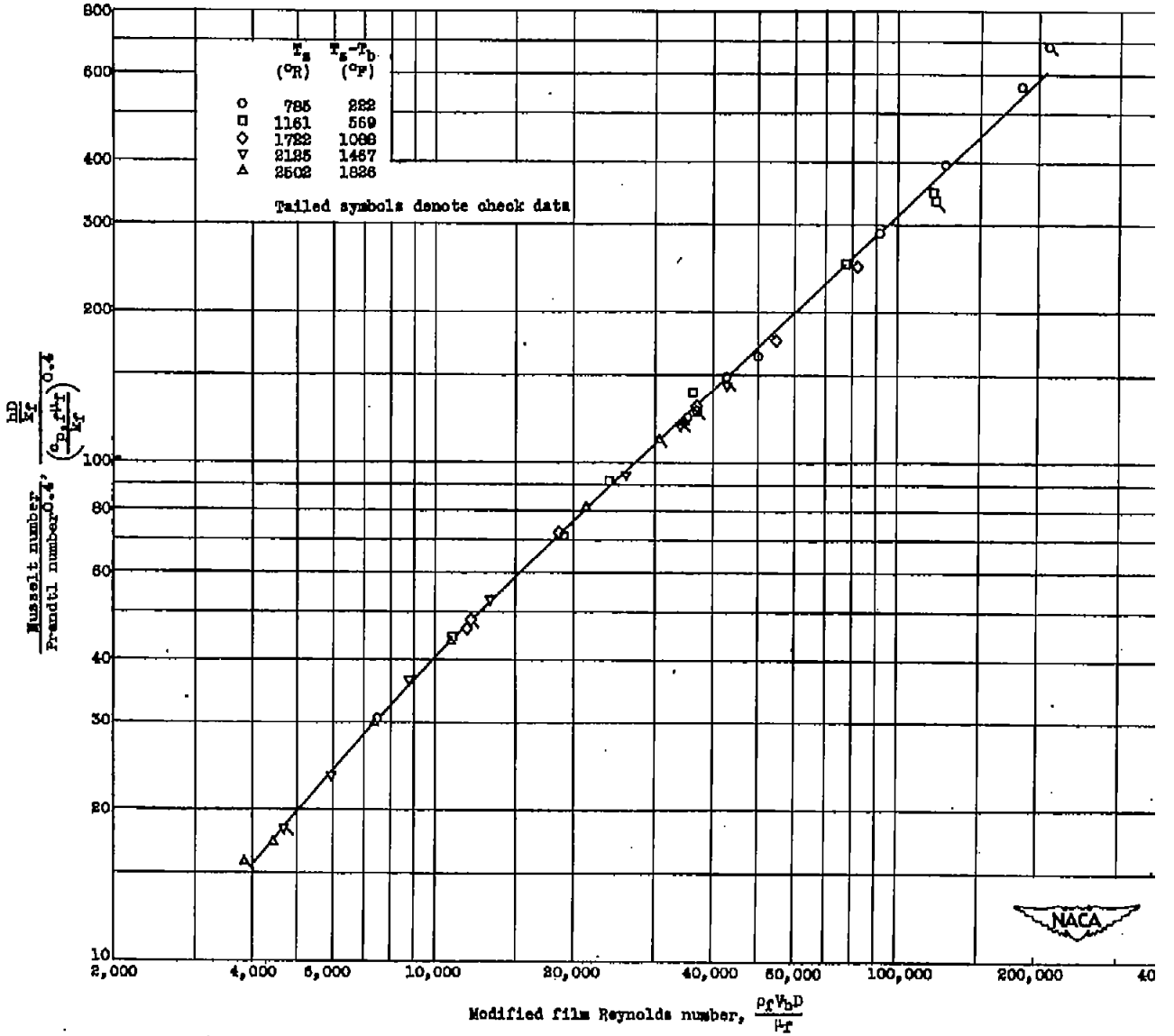

Figure 13. - Correlation of heat-transfer data using modified film Reynolds number. Physical properties of air evaluate at average film temperature T_f.

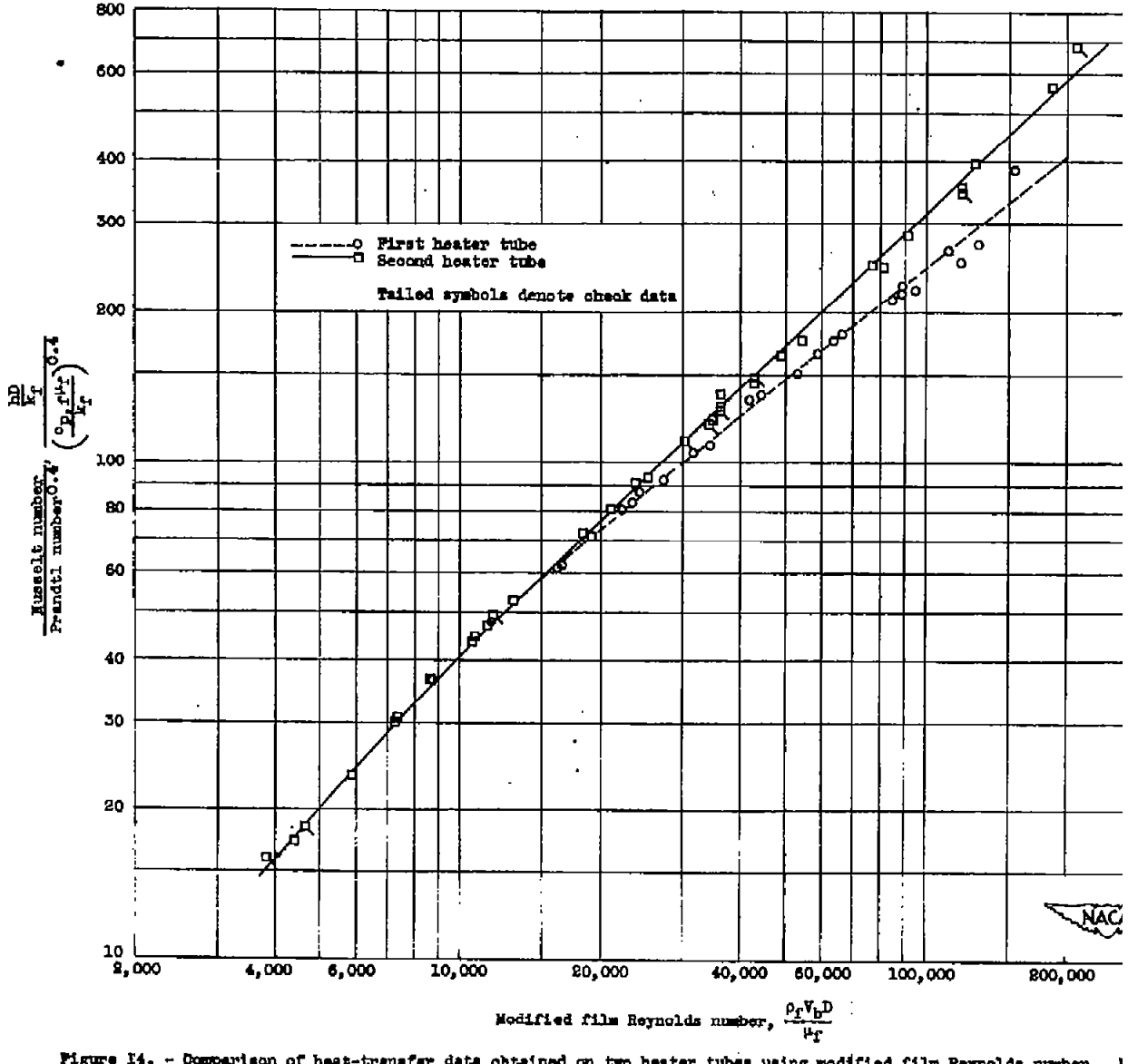

Figure 14. - Comparison of heat-transfer data obtained on two heater tubes using modified film Reynolds number. I properties of air evaluated at average film temperature T_f.

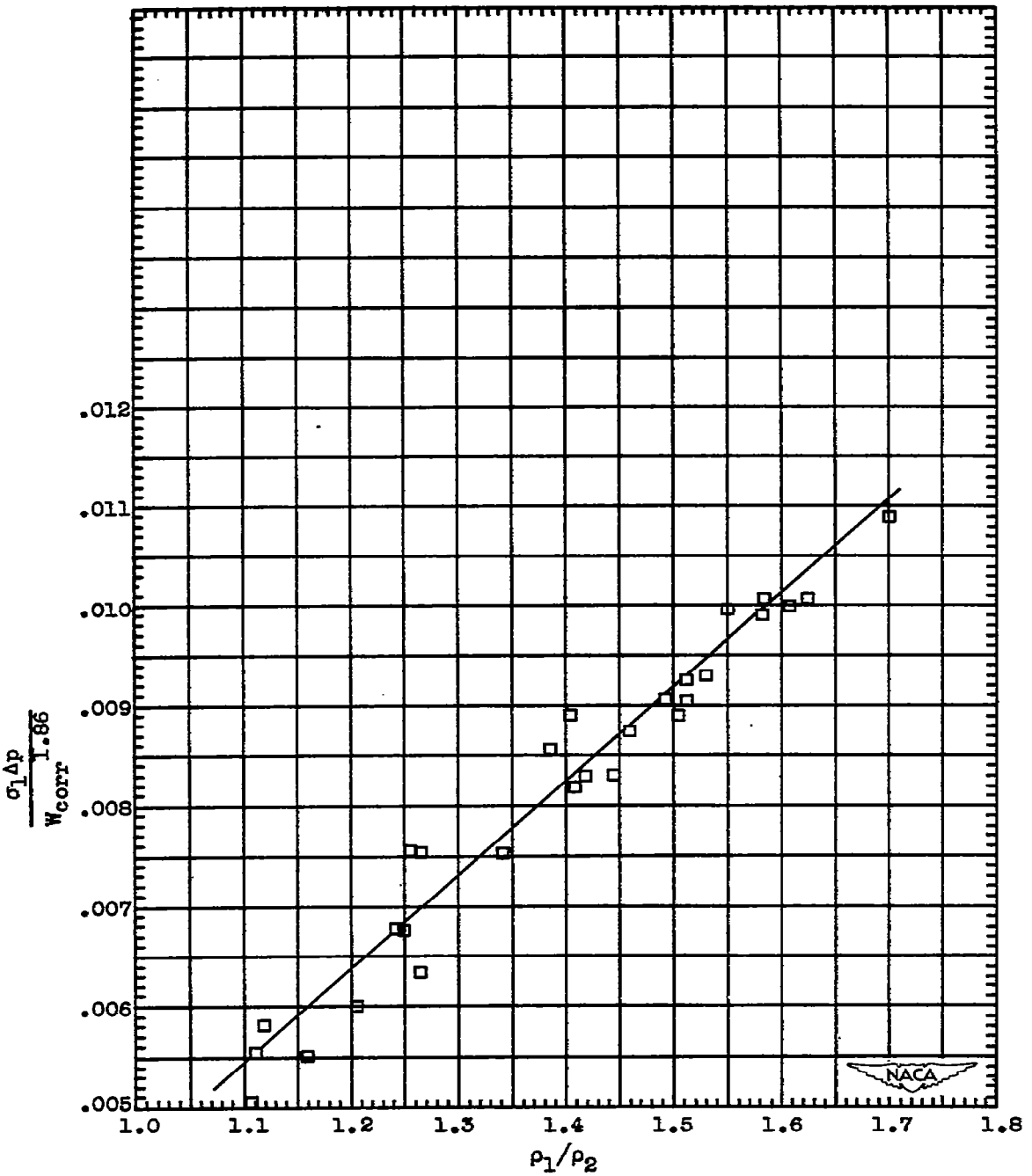

Figure 15. - Correlation of measured static-pressure drop through heater tube for various values of air flow and heat-transfer rate. Data from second heater tube.